Ukrainian Journal of Physical Optics
ISSUE 3
2026

INVESTIGATION OF NEW OPTICAL SOLUTIONS OF THE FRACTIONAL SCHRÖDINGER EQUATION WITH ACCOUNTING FOR THIRD-ORDER NONLINEARITY

SOFIAN T. OBIEDAT [1], DOAA RIZK [2,*], WAEL W MOHAMMED [1]

[1] Department of Mathematics, College of Science, University of Ha'il, Ha'il 2440, Saudi Arabia
[2] Department of Mathematics, College of Science, Qassim University, Buraydah, 51452, Saudi Arabia
* Corresponding author: d.hussien@qu.edu.sa

Received: 21.03.2026

Abstract. In this paper, we consider the quadratic–cubic nonlinear Schrödinger equation (QC-NLSE) formulated with the M-truncated derivative (MTD). By employing the F-expansion method, a variety of exact analytical solutions are obtained, including periodic, bright, kink, anti-kink, singular, and dark soliton structures. The method is shown to be systematic and effective for constructing exact solutions of nonlinear evolution equations with fractional-order characteristics. The main contribution of this work is the derivation and classification of a diverse family of wave solutions to the QC-NLSE using MTD. Graphical simulations are performed using MATLAB to illustrate the influence of the fractional parameter on the behavior of the obtained solutions. The results demonstrate that variations in this parameter lead to noticeable changes in the shape and propagation characteristics of the wave structures, while the analytical method serves to describe these properties.

Keywords: M-truncated derivative, optical solitons, simulation, F-expansion method, quadratic-cubic nonlinear evolution equations
UDC: 517.958; 530.145; 517.977; 517.955
DOI: 10.3116/16091833/Ukr.J.Phys.Opt.2026.03083

1. Introduction

Fractional nonlinear evolution equations (FNLEEs) provide a powerful mathematical framework for studying complex systems with memory effects and nonlinear interactions, yielding novel insights and applications in engineering and science [1-5]. The non-linear nature of these equations makes them suitable for modeling an extensive range of phenomena in engineering, biology, chemistry, and physics. As a result, it is significant to solve these FNLEEs. Recently, various powerful techniques for finding exact solutions to FNLEEs have been presented, such as the $\exp(-\phi(\xi))$-expansion method [6], the sine-Gordon expansion technique [7], the Jacobi elliptic function expansion method [8], the F-expansion method [9], the Riccati equation method [10], the exp-function method [11], the (G'/G)-expansion method [12, 13], and the sine-cosine method [14], etc.

In recent years, several fractional operators, such as the Caputo, Riemann–Liouville, and Atangana–Baleanu derivatives, have been widely employed to model memory and hereditary effects in nonlinear systems. Despite their effectiveness, these operators present certain limitations. For instance, the Riemann–Liouville derivative often poses difficulties in prescribing physically meaningful initial conditions, whereas the Caputo derivative, although more suitable in this regard, may impose analytical constraints when solving nonlinear problems. On the other hand, the Atangana–Baleanu derivative introduces a nonlocal,

nonsingular kernel, which enhances modeling capabilities but increases computational and analytical complexity.

The fractional quadratic-cubic nonlinear Schrödinger equation (FQC-NLSE) is a mathematical equation that explains the behavior of wave functions in certain physical systems. This equation combines elements of quantum mechanics, nonlinear dynamics, and fractional calculus to provide a more accurate representation of complex systems. The quadratic-cubic nonlinearity term in the equation accounts for particle interactions in the system and enables the study of phenomena such as solitons and rogue waves.

On the other side, the fractional quadratic–cubic nonlinear Schrödinger equation (QC-NLSE) has attracted considerable attention, and a variety of analytical approaches have been developed to explore its solution structures. For instance, Attia et al. [15] investigated the space–time fractional QC-NLSE with the Atangana–Baleanu derivative using the modified Khater and generalized $\exp\left(-\phi(\xi)\right)$-expansion methods, while Badshah et al. [16] employed the unified method and the extended simple equation method to obtain exact solutions for the same model. In a different direction, Islam et al. [17] considered the conformable fractional QC-NLSE and derived analytical solutions via the improved tanh method and the rational (G'/G) -expansion technique. Although these studies have significantly advanced the understanding of fractional QC-NLSE models, they are primarily restricted to specific fractional operators and solution techniques.

The QC-NLSE with M-truncated derivative (QC-NLSE-MTD) under consideration is written as [15-17]:

$$iM_t^{\beta,\delta}u + a_1 u_{xx} - a_2|u|u + a_3|u|^2 u = 0, \tag{1}$$

where $u = u(x,t)$ is a complex-valued wave function depending on the spatial variable x and temporal variable t. The operator $M_t^{\beta,\delta}$ denotes the M-truncated derivative with respect to time, which provides a generalized description of temporal evolution and can be used to incorporate memory effects and nonlocal temporal behavior into the model. The coefficient a_1 represents the group velocity dispersion, while a_2 and a_3 are the strengths of the quadratic and cubic nonlinear terms, respectively. The quadratic nonlinear term $-a_2|u|u$ is associated with second-order nonlinear effects, such as three-wave mixing processes (e.g., second-harmonic generation). The cubic nonlinear term $a_3|u|^2 u$ accounts for Kerr-type nonlinearity, which can describe either self-focusing or self-defocusing behavior depending on the sign of a_3.

However, the use of the M-truncated derivative (MTD) in the context of the QC-NLSE has not yet been adequately explored. This reveals a clear gap in the literature, particularly regarding the development of exact solutions within alternative fractional frameworks that may offer improved analytical tractability and greater flexibility in describing nonlinear wave phenomena. Motivated by this gap, the present study considers the time-fractional QC-NLSE with the M-truncated derivative and applies the F-expansion method to construct a broad class of exact solutions. This approach not only complements existing results but also extends the current body of knowledge by introducing a different fractional operator and solution framework for the QC-NLSE.

The main aim of this study is to obtain exact solutions to the QC-NLSE-MTD (1). Solutions in the type of rational, elliptic, trigonometric, and hyperbolic functions can be produced using the F-expansion approach. To address the influence of the MTD on the acquired solutions of Eq. (1), several graphs are also produced using the MATLAB tool.

The paper's outline is as follows: We define MTD and list its properties in Section 2, while the QC-NLSE-MTD wave Eq. (1) is described in Section 3. After that, in Section 4, we obtain the solutions of QC-NLSE-MTD (1) and plot figures to examine the influence of MTD on the solutions. In Section 5, we present the physical interpretation of the solutions obtained. The conclusion of the study is stated in the end.

2. The M-truncated derivative

Since fractional derivative operators are more effective than integer order derivatives for simulating the behavior of complex systems, they are crucial in many fields of science and engineering. Many types of fractional derivative operators are available, such as the Katugampola derivative, Jumarie derivative, Caputo derivative, Hadamard derivative, and Grünwald-Letnikov derivative, Riemann-Liouville derivative [18-21]. A new derivative, defined as the M-truncated derivative (MTD), was recently introduced by Sousa et al. [22]. This derivative naturally evolves from the classic derivative. The MTD incorporates classic calculus properties such as linearity, the product rule, the quotient rule, the composition rule, and the chain rule.

Definition: Let $u:[a,\infty)\to\mathbb{R}$ be a continuous function. Then the MTD of order $0<\beta\le 1$ is defined by: $M_t^{\beta,\delta}u(t)=\lim_{h\to 0}\frac{u\left(tE_\delta(ht^{-\beta})\right)-u(t)}{h}$, where $h\in\mathbb{R}$ is an increment parameter and $\delta>0$. The function $E_\delta(\cdot)$ denotes the truncated Mittag–Leffler-type function defined by $E_\delta(Q)=\sum_{k=0}^{n}\frac{Q^k}{\Gamma(k\delta+1)}$, $Q\in\mathbb{C}$, where k is the summation index, $n\in\mathbb{N}$ determines the truncation order, and $\Gamma(\cdot)$ is the Gamma function.

Theorem: Consider $f(t)$ and $g(t)$ that are β-order differentiable, then the MTD satisfies the following features for any real constants a and b [22]:

$$M_t^{\beta,\delta}\left(af(t)+bg(t)\right)=aM_t^{\beta,\delta}f(t)+bM_t^{\beta,\delta}g(t),\quad M_t^{\beta,\delta}\left(t^n\right)=\frac{n}{\Gamma(\beta+1)}t^{n-\beta},$$

$$M_t^{\beta,\delta}\left(f(t)g(t)\right)=f(t)M_t^{\beta,\delta}g(t)+g(t)M_t^{\beta,\delta}f(t),$$

$$M_t^{\beta,\delta}f(t)=\frac{t^{1-\beta}}{\Gamma(\beta+1)}\frac{df}{dt},\quad M_t^{\beta,\delta}(f\circ g)(t)=f'\left(g(t)\right)M_t^{\beta,\delta}f(t).$$

3. Traveling wave equation for the QC-NLSE-MTD

The QC-NLSE-MTD wave Eq. (1) is obtained by applying

$$u(x,\,t)=Q(\rho)e^{i\theta},\tag{2}$$

where Q is the real-valued amplitude profile, and θ is the phase. The variables ρ and θ describe a traveling wave structure with fractional temporal evolution. The wave variables ρ and θ are defined by

$$\rho=kx+\frac{\lambda\Gamma(\delta+1)}{\beta}t^\beta,\text{ and }\theta=\theta_1x+\frac{\theta_2\Gamma(\delta+1)}{\beta}t^\beta,$$

where k, λ, θ_1, and θ_2 are the wave number, wave velocity, spatial frequency of the phase,

and temporal frequencies of the phase, respectively. We note that

$$M_t^{\beta,\delta}u=\left[\lambda Q'+i\theta_2 Q\right]e^{i\theta}\text{, and } u_{xx}=\left[k^2Q''+2ik\theta_1Q'-\theta_1^2Q\right]e^{i\theta}, \tag{3}$$

where $Q'=\dfrac{dQ}{d\rho}$ and $Q''=\dfrac{d^2Q}{d\rho^2}$. Plugging Eqs. (2) and (3) into Eq. (1), we get for the real part

$$a_1k^2Q''-\left(a_1\theta_1^2+\theta_2\right)Q-a_2Q^2+a_3Q^3=0, \tag{4}$$

and for the imaginary part

$$Q'\left(\lambda+2ka_1\theta_1\right)=0. \tag{5}$$

Let

$$\lambda=-2ka_1\theta_1, \tag{6}$$

which gives the velocity of the travelling wave.

Rewriting Eq. (4) as follows

$$Q''+A_1Q+A_2Q^2+A_3Q^3=0, \tag{7}$$

where $A_1=\dfrac{-\left(a_1\theta_1^2+\theta_2\right)}{a_1k^2}$, $A_2=\dfrac{-a_2}{a_1k^2}$, and $A_3=\dfrac{a_3}{a_1k^2}$.

4. Exact solutions of the QC-NLSE-MTD

Let us utilize the F-expansion method (for more information, see [23-24]). Assuming the solution of Eq. (7) is

$$Q(\rho)=\sum_{i=0}^{m}\ell_i F^i(\rho), \tag{8}$$

where $\ell_1, \ell_2, \ell_3,\ldots\ldots, \ell_{m-1}$ and $\ell_m\neq 0$ are unknown constants to be computed. The coefficients ℓ_i are amplitude parameters that determine the contribution of each power of the auxiliary function $F(\rho)$ to the wave profile. They control the shape, localization, and nonlinear characteristics of the solution, such as its amplitude, width, and type. While F solves the auxiliary equation:

$$\left(F'\right)^2=h_1F^4+h_2F^2+h_3, \tag{9}$$

where h_1, h_2, and h_3 are real constants that determine the qualitative behavior of the auxiliary function $F(\rho)$. They control the type of solutions obtained (solitary, periodic, or elliptic) and are indirectly related to the system's physical properties through the balance between nonlinearity and dispersion.

First, let us equate Q^3 with Q'' in Eq. (7) to compute the parameters m as $3m=m+2\Rightarrow m=1.$ With $m=1$, Eq. (8) becomes

$$Q(\rho)=\ell_0+\ell_1F(\rho), \tag{10}$$

Putting Eq. (10) into Eq. (7) and using Eq. (9), we get

$$\left[2h_1\ell_1+\mathrm{A}_3\ell_1^3\right]F^3+\left[\mathrm{A}_2\ell_1^2+3\mathrm{A}_3\ell_0\ell_1^2\right]F^2+\left[h_2\ell_1+\mathrm{A}_1\ell_1+2\ell_0\ell_1\mathrm{A}_2+3\mathrm{A}_2\ell_0^2\ell_1\right]F$$
$$+\left[\mathrm{A}_1\ell_0+\mathrm{A}_2\ell_0^2+\mathrm{A}_3\ell_0^3\right]=0.$$

For $i=3,2,1,0$, we balance each coefficient of F^i with zero to have $2h_1\ell_1+\mathrm{A}_3\ell_1^3=0$, $\mathrm{A}_2\ell_1^2+3\mathrm{A}_3\ell_0\ell_1^2=0$, $h_2\ell_1+\mathrm{A}_1\ell_1+2\ell_0\ell_1\mathrm{A}_2+3\mathrm{A}_2\ell_0^2\ell_1=0$, and $\mathrm{A}_1\ell_0+\mathrm{A}_2\ell_0^2+\mathrm{A}_3\ell_0^3=0.$

By solving the above equations, we have

$$\ell_0=\frac{-\mathrm{A}_2}{3\mathrm{A}_3}=\frac{\mathrm{a}_2}{3\mathrm{a}_3},\ \ell_1=\pm\sqrt{\frac{-2h_1}{\mathrm{A}_3}}=\pm\sqrt{\frac{-2k^2\mathrm{a}_1h_1}{\mathrm{a}_3}},\ \text{and}$$

$$h_2=\frac{A_2^2}{9\mathrm{A}_3}=\frac{\mathrm{a}_2}{9k^2\mathrm{a}_1\mathrm{a}_3}. \tag{11}$$

Substituting Eq. (11) into Eq. (10), we have the solution of the traveling wave Eq. (7) as:

$$Q(\rho)=\frac{\mathrm{a}_2}{3\mathrm{a}_3}\pm\sqrt{\frac{-2\mathrm{a}_2h_1}{9\mathrm{h}_2a_3^2}}F(\rho). \tag{12}$$

Consequently, putting Eq. (12) into Eq. (2), we get the following solutions for the QC-NLSE-MTD (1):

$$u(x,t)=\left(\frac{\mathrm{a}_2}{3\mathrm{a}_3}\pm\sqrt{\frac{-2\mathrm{a}_2h_1}{9\mathrm{h}_2a_3^2}}F(\rho)\right)e^{i\theta}. \tag{13}$$

There are several cases for the solutions of that Eq. (9) depend on h_1,h_2 and h_3 as follows:

Case 1: If $h_1=\varpi^2, h_2=-(1+\varpi^2)$ and $h_3=1$, then $F(\rho)=sn(\rho;\varpi)$, where the parameter ϖ is the elliptic modulus of the Jacobi elliptic function, which controls the shape of the solution. In this case, Eq. (13) takes the form

$$\begin{aligned}u(x,t)=&\left(\frac{\mathrm{a}_2}{3\mathrm{a}_3}\pm\sqrt{\frac{2\mathrm{a}_2\varpi^2}{9(1+\varpi^2)a_3^2}}sn\left(kx+\frac{\lambda\Gamma(\delta+1)}{\beta}t^\beta;\varpi\right)\right)\\&\times\exp\left[i\left(\theta_1x+\frac{\theta_2\Gamma(\delta+1)}{\beta}t^\beta\right)\right].\end{aligned} \tag{14}$$

This solution represents a nonlinear periodic wave, in which ϖ controls the transition from sinusoidal behavior to soliton behavior. When $\varpi\to1$, Eq. (14) (see Table 1) reduces to:

$$\begin{aligned}u(x,t)=&\left(\frac{\mathrm{a}_2}{3\mathrm{a}_3}\pm\sqrt{\frac{\mathrm{a}_2}{9a_3^2}}tanh\left(kx+\frac{\lambda\Gamma(\delta+1)}{\beta}t^\beta\right)\right)\\&\times\exp\left[i\left(\theta_1x+\frac{\theta_2\Gamma(\delta+1)}{\beta}t^\beta\right)\right],\end{aligned} \tag{15}$$

while this solution represents a localized solitary wave (kink-type soliton) described by the hyperbolic tangent function.

Case 2: If $h_1=-\varpi^2, h_2=2\varpi^2-1$ and $h_3=1-\varpi^2$, then $F(\rho)=cn(\rho;\varpi)$. In this case, Eq. (13) takes the form:

$$\begin{aligned}u(x,t)=&\left(\frac{\mathrm{a}_2}{3\mathrm{a}_3}\pm\sqrt{\frac{2\mathrm{a}_2\varpi^2}{9(2\varpi^2-1)a_3^2}}cn\left(kx+\frac{\lambda\Gamma(\delta+1)}{\beta}t^\beta;\varpi\right)\right)\\&\times\exp\left[i\left(\theta_1x+\frac{\theta_2\Gamma(\delta+1)}{\beta}t^\beta\right)\right],\end{aligned} \tag{16}$$

for $<1/\sqrt{2}$. This solution represents a nonlinear periodic wave, where the elliptic modulus ϖ controls the transition from periodic wave trains to soliton-like structures. When $\varpi\to1$, Eq. (16) (see Table 1) turns to:

$$u(x,t)=\left(\frac{a_2}{3a_3}\pm\sqrt{\frac{2a_2}{9a_3^2}}\operatorname{sech}\left(kx+\frac{\lambda\Gamma(\delta+1)}{\beta}t^{\beta}\right)\right)\times\exp\left[i\left(\theta_1 x+\frac{\theta_2\Gamma(\delta+1)}{\beta}t^{\beta}\right)\right]. \tag{17}$$

This solution represents a localized, bright solitary wave (sech-type soliton) with a stable envelope that propagates in the medium.

Case 3: If $h_1=-1$, $h_2=2-\varpi^2$ and $h_3=\varpi^2-1$, then $F(\rho)=dn(\rho;\varpi)$. In this case Eq. (13) takes the form:

$$u(x,t)=\left(\frac{a_2}{3a_3}\pm\sqrt{\frac{2a_2}{9(2-\varpi^2)a_3^2}}dn\left(kx+\frac{\lambda\Gamma(\delta+1)}{\beta}t^{\beta};\varpi\right)\right)\exp\left[i\left(\theta_1 x+\frac{\theta_2\Gamma(\delta+1)}{\beta}t^{\beta}\right)\right]. \tag{18}$$

This solution represents a nonlinear periodic wave, where ϖ controls the transition between periodic and soliton-like behavior. If $\varpi\to 1$, then Eq. (18) transfer to Eq. (17).

Case 4: If $h_1=1$, $h_2=-(\varpi^2+1)$ and $h_3=\varpi^2$, then $F(\rho)=ns(\rho;\varpi)$. In this case, Eq. (13) takes the form:

$$u(x,t)=\left(\frac{a_2}{3a_3}\pm\sqrt{\frac{2a_2}{9(\varpi^2+1)a_3^2}}ns\left(kx+\frac{\lambda\Gamma(\delta+1)}{\beta}t^{\beta};\varpi\right)\right)\times\exp\left[i\left(\theta_1 x+\frac{\theta_2\Gamma(\delta+1)}{\beta}t^{\beta}\right)\right]. \tag{19}$$

This solution represents a nonlinear periodic wave expressed in terms of Jacobi elliptic functions, corresponding to a modulated wave train whose profile is governed by the elliptic modulus ϖ. When $\varpi\to 1$, Eq. (19) (see Table 1) becomes

$$u(x,t)=\left(\frac{a_2}{3a_3}\pm\sqrt{\frac{a_2}{9a_3^2}}\coth\left(kx+\frac{\lambda\Gamma(\delta+1)}{\beta}t^{\beta}\right)\right)\times\exp\left[i\left(\theta_1 x+\frac{\theta_2\Gamma(\delta+1)}{\beta}t^{\beta}\right)\right]. \tag{20}$$

While this solution represents a localized singular solitary wave (coth-type kink solution), exhibiting a sharp transition structure propagating in the medium. When $\varpi\to 1$, Eq. (19) (see Table 1) reduces to:

$$u(x,t)=\left(\frac{a_2}{3a_3}\pm\sqrt{\frac{2a_2}{9a_3^2}}\csc\left(kx+\frac{\lambda\Gamma(\delta+1)}{\beta}t^{\beta}\right)\right)\times\exp\left[i\left(\theta_1 x+\frac{\theta_2\Gamma(\delta+1)}{\beta}t^{\beta}\right)\right]. \tag{21}$$

This solution represents a nonlinear periodic wave with singular behavior, corresponding to a csc-type periodic structure with oscillatory profiles in the medium.

Case 5: If $h_1=1$, $h_2=-(\varpi^2+1)$ and $h_3=\varpi^2$, then $F(\rho)=dc(\rho;\varpi)=\frac{dn(\rho;\varpi)}{cn(\rho;\varpi)}$. In this case, Eq. (13) takes the form:

$$u(x,t)=\left(\frac{a_2}{3a_3}\pm\sqrt{\frac{2a_2}{9(\varpi^2+1)a_3^2}}dc\left(kx+\frac{\lambda\Gamma(\delta+1)}{\beta}t^{\beta};\varpi\right)\right)\times\exp\left[i\left(\theta_1 x+\frac{\theta_2\Gamma(\delta+1)}{\beta}t^{\beta}\right)\right]. \tag{22}$$

This solution (22) represents a nonlinear periodic wave expressed in terms of Jacobi elliptic functions, corresponding to a modulated wave train. The elliptic modulus ϖ controls the wave profile and its transition toward soliton-like behavior. When $\varpi\to 1$, Eq. (22) (see Table 1) reduces to:

$$u(x,t)=\left(\frac{a_2}{3a_3}\pm\sqrt{\frac{2a_2}{9a_3^2}}sec\left(kx+\frac{\lambda\Gamma(\delta+1)}{\beta}t^{\beta}\right)\right)\times\exp\left[i\left(\theta_1 x+\frac{\theta_2\Gamma(\delta+1)}{\beta}t^{\beta}\right)\right]. \tag{23}$$

While the solution (23) represents a nonlinear periodic wave with singular behavior, described by a sec-type profile, corresponding to an oscillatory wave structure with sharp peaks in the medium.

Case 6: If $h_1=1-\varpi^2$, $h_2=2\varpi^2-1$ and $h_3=-\varpi^2$, then $F(\rho)=nc(\rho;\varpi)$. In this case, Eq. (13) takes the form:

$$u(x,t)=\left(\frac{a_2}{3a_3}\pm\sqrt{\frac{2a_2(1-\varpi^2)}{9(1-2\varpi^2)a_3^2}}nc\left(kx+\frac{\lambda\Gamma(\delta+1)}{\beta}t^{\beta};\varpi\right)\right)\times\exp\left[i\left(\theta_1 x+\frac{\theta_2\Gamma(\delta+1)}{\beta}t^{\beta}\right)\right], \tag{23}$$

for $0<\varpi<1/\sqrt{2}$. The solution (24) represents a nonlinear periodic (elliptic) wave of nc-type, describing a modulated wave train. The elliptic modulus ϖ controls the wave profile and its transition between periodic and soliton-like behavior. If $\varpi\to 0$, then Eq. (24) transfer to Eq. (23).

Case 7: If $h_1=\varpi^2-1$, $h_2=2-\varpi^2$ and $h_3=-1$, then $F(\rho)=nd(\rho;\varpi)$. In this case, Eq. (13) takes the form:

$$u(x,t)=\left(\frac{a_2}{3a_3}\pm\sqrt{\frac{2a_2(1-\varpi^2)}{9(2-\varpi^2)a_3^2}}nc\left(kx+\frac{\lambda\Gamma(\delta+1)}{\beta}t^{\beta};\varpi\right)\right)\times\exp\left[i\left(\theta_1 x+\frac{\theta_2\Gamma(\delta+1)}{\beta}t^{\beta}\right)\right]. \tag{25}$$

The solution represents a nonlinear periodic (elliptic) nc-type wave, corresponding to a modulated wave train. The elliptic modulus ϖ governs the wave profile and controls the transition between periodic and soliton-like structures.

Case 8: If $h_1=-\varpi^2(1-\varpi^2)$, $h_2=2\varpi^2-1$ and $h_3=1$, then $F(\rho)=sd(\rho;\varpi)$. In this case Eq. (13) takes the form:

$$u(x,t)=\left(\frac{a_2}{3a_3}\pm\sqrt{\frac{2a_2\varpi^2(1-\varpi^2),}{9(2\varpi^2-1)a_3^2}}sd\left(kx+\frac{\lambda\Gamma(\delta+1)}{\beta}t^{\beta};\varpi\right)\right)\times\exp\left[i\left(\theta_1 x+\frac{\theta_2\Gamma(\delta+1)}{\beta}t^{\beta}\right)\right], \tag{26}$$

for $>1/\sqrt{2}$. The solution (26) represents a nonlinear periodic (elliptic) wave of sd-type, describing a modulated wave train. The elliptic modulus ϖ controls the wave profile and

governs the transition between periodic and soliton-like behavior.

Case 9: If $h_1=1$, $h_2=2\varpi^2-1$ and $h_3=-\varpi^2(1-\varpi^2)$, then $F(\rho)=ds(\rho;\varpi)$. In this case, Eq. (13) takes the form:

$$u(x,t)=\left(\frac{a_2}{3a_3}\pm\sqrt{\frac{2a_2,}{9(1-2\varpi^2)a_3^2}}ds\left(kx+\frac{\lambda\Gamma(\delta+1)}{\beta}t^\beta;\varpi\right)\right)\times\exp\left[i\left(\theta_1 x+\frac{\theta_2\Gamma(\delta+1)}{\beta}t^\beta\right)\right], \tag{27}$$

for $<1/\sqrt{2}$. This solution represents a nonlinear periodic wave expressed in terms of Jacobi elliptic functions, in which the elliptic modulus ϖ governs the transition between periodic and soliton-like wave structures.

Case 10: If $h_1=1/4$, $h_2=(\varpi^2-2)/2$ and $h_3=\varpi^2/4$, then $F(\rho)=ns(\rho;\varpi)+ds(\rho;\varpi)$. In this case Eq. (13) takes the form:

$$u(x,t)=\left[\frac{a_2}{3a_3}\pm\sqrt{\frac{a_2,}{9(2-\varpi^2)a_3^2}}\left(\begin{array}{l}ns\left(kx+\frac{\lambda\Gamma(\delta+1)}{\beta}t^\beta;\varpi\right)\\+ds\left(kx+\frac{\lambda\Gamma(\delta+1)}{\beta}t^\beta;\varpi\right)\end{array}\right)\right]\times\exp\left[i\left(\theta_1 x+\frac{\theta_2\Gamma(\delta+1)}{\beta}t^\beta\right)\right]. \tag{28}$$

When $\varpi\to 1$, Eq. (28) (see Table 1) turns to:

$$u(x,t)=\left[\frac{a_2}{3a_3}\pm\sqrt{\frac{a_2,}{9a_3^2}}\left(\begin{array}{l}coth\left(kx+\frac{\lambda\Gamma(\delta+1)}{\beta}t^\beta\right)\\csch\left(kx+\frac{\lambda\Gamma(\delta+1)}{\beta}t^\beta\right)\end{array}\right)\right]\times\exp\left[i\left(\theta_1 x+\frac{\theta_2\Gamma(\delta+1)}{\beta}t^\beta\right)\right]. \tag{29}$$

The solution (29) represents a localized singular solitary wave composed of hyperbolic functions (coth–csch type), describing a sharply varying kink-like structure with singular behavior propagating in the medium. When $\varpi\to 1$, Eq. (28) (see Table 1) reduces to:

$$u(x,t)=\left[\frac{a_2}{3a_3}\pm\sqrt{\frac{a_2,}{18a_3^2}}\left(\begin{array}{l}csc\left(kx+\frac{\lambda\Gamma(\delta+1)}{\beta}t^\beta\right)\\+cot\left(kx+\frac{\lambda\Gamma(\delta+1)}{\beta}t^\beta\right)\end{array}\right)\right]\times\exp\left[i\left(\theta_1 x+\frac{\theta_2\Gamma(\delta+1)}{\beta}t^\beta\right)\right]. \tag{30}$$

While the solution (30) represents a nonlinear periodic wave with singular behavior, expressed through trigonometric functions (csc–cot type), corresponding to an oscillatory wave profile with periodic singular structures.

Case 11: If $h_1=\frac{\varpi^2}{4}$, $h_2=\frac{\varpi^2-2}{2}$ and $h_3=\frac{\varpi^2}{4}$, then $F(\rho)=\sqrt{1-\varpi^2}\left(sd(\rho;\varpi)+cd(\rho;\varpi)\right)$. In this case, Eq. (13) takes the form:

$$u(x,t)=\left[\frac{a_2}{3a_3}\pm\sqrt{\frac{a_2,\varpi^2(1-\varpi^2)}{9(2-\varpi^2)a_3^2}}\left(\begin{array}{l}sd\left(kx+\dfrac{\lambda\Gamma(\delta+1)}{\beta}t^\beta;\varpi\right)\\+cd\left(kx+\dfrac{\lambda\Gamma(\delta+1)}{\beta}t^\beta;\varpi\right)\end{array}\right)\right]\times\exp\left[i\left(\theta_1 x+\frac{\theta_2\Gamma(\delta+1)}{\beta}t^\beta\right)\right]. \tag{31}$$

Case 12: If $h_1=\frac{\varpi^2-1}{4}$, $h_2=\frac{\varpi^2+1}{2}$ and $h_3=\frac{\varpi^2-1}{4}$, then $F(\rho)=\varpi sd(\rho;\varpi)+nd(\rho;\varpi)$. In this case, Eq. (13) takes the form:

$$u(x,t)=\left[\frac{a_2}{3a_3}\pm\sqrt{\frac{a_2(1-\varpi^2)}{9(1+\varpi^2)a_3^2}}\left(\begin{array}{l}\varpi sd\left(kx+\dfrac{\lambda\Gamma(\delta+1)}{\beta}t^\beta;\varpi\right)\\+nd\left(kx+\dfrac{\lambda\Gamma(\delta+1)}{\beta}t^\beta;\varpi\right)\end{array}\right)\right]\times\exp\left[i\left(\theta_1 x+\frac{\theta_2\Gamma(\delta+1)}{\beta}t^\beta\right)\right]. \tag{32}$$

The solution (32) represents a nonlinear periodic wave constructed from Jacobi elliptic functions and describes a modulated wave train. The elliptic modulus ϖ controls the wave profile and its transition toward soliton-like behavior.

Case 13: If $h_1=\frac{\varpi^2}{4}$, $h_2=\frac{\varpi^2-2}{2}$ and $h_3=\frac{1}{4}$, then $F(\rho)=\frac{sn(\rho;\varpi)}{1+dn(\rho;\varpi)}$. In this case, Eq. (13) takes the form:

$$u(x,t)=\left(\frac{a_2}{3a_3}\pm\sqrt{\frac{a_2\varpi^2}{9(2-\varpi^2)a_3^2}}\frac{sn\left(kx+\dfrac{\lambda\Gamma(\delta+1)}{\beta}t^\beta;\varpi\right)}{1+dn\left(kx+\dfrac{\lambda\Gamma(\delta+1)}{\beta}t^\beta;\varpi\right)}\right)\times\exp\left[i\left(\theta_1 x+\frac{\theta_2\Gamma(\delta+1)}{\beta}t^\beta\right)\right]. \tag{33}$$

The solution (33) represents a nonlinear periodic (elliptic) wave expressed in terms of Jacobi elliptic functions, describing a modulated wave train. The elliptic modulus ϖgoverns the transition between periodic and soliton-like structures. When ϖ→1, Eq. (33) (see Table 1) reduces to:

$$u(x,t)=\left(\frac{a_2}{3a_3}\pm\sqrt{\frac{a_2}{9a_3^2}}\frac{tanh\left(kx+\dfrac{\lambda\Gamma(\delta+1)}{\beta}t^\beta\right)}{1+sech\left(kx+\dfrac{\lambda\Gamma(\delta+1)}{\beta}t^\beta\right)}\right)\times\exp\left[i\left(\theta_1 x+\frac{\theta_2\Gamma(\delta+1)}{\beta}t^\beta\right)\right]. \tag{34}$$

The solution (34) represents a localized nonlinear solitary wave (kink-type structure) with a modified hyperbolic profile. It describes a stable wave packet whose shape is governed by the balance between nonlinearity and dispersion.

Case 14: If $h_1=-(1/4)$, $h_2=(\varpi^2+1)/2$ and $h_3=(\varpi^2-1)^2/4$, then $F(\rho)=\varpi cn(\rho;\varpi)+dn(\rho;\varpi)$. In this case, Eq. (13) takes the form:

$$u(x,t)=\left[\frac{a_2}{3a_3}\pm\sqrt{\frac{a_2}{9(1+\varpi^2)a_3^2}}\left(\begin{array}{l}\varpi cn\left(kx+\dfrac{\lambda\Gamma(\delta+1)}{\beta}t^{\beta};\varpi\right)\\+dn\left(kx\dfrac{\lambda\Gamma(\delta+1)}{\beta}t^{\beta};\varpi\right)\end{array}\right)\right]\times\exp\left[i\left(\theta_1 x+\frac{\theta_2\Gamma(\delta+1)}{\beta}t^{\beta}\right)\right] \tag{35}$$

This solution (35) represents a nonlinear periodic (elliptic) wave formed by a superposition of Jacobi functions cn and dn. The elliptic modulus ϖ controls the wave profile, governing the transition between periodic wave trains and soliton-like structures.

Case 15: If $h_1=1$, $h_2=2-4\varpi^2$ and $h_3=1$, then $F(\rho)=\dfrac{sn(\rho;\varpi)dn(\rho;\varpi)}{cn(\rho;\varpi)}$. In this case, Eq. (13) takes the form:

$$u(x,t)=\left(\begin{array}{l}\dfrac{a_2}{3a_3}\pm\sqrt{\dfrac{a_2}{9(2\varpi^2-1)a_3^2}}\\\times\dfrac{sn\left(kx+\dfrac{\lambda\Gamma(\delta+1)}{\beta}t^{\beta};\varpi\right)dn\left(kx+\dfrac{\lambda\Gamma(\delta+1)}{\beta}t^{\beta};\varpi\right)}{cn\left(kx+\dfrac{\lambda\Gamma(\delta+1)}{\beta}t^{\beta};\varpi\right)}\end{array}\right)\times\exp\left[i\left(\theta_1 x+\frac{\theta_2\Gamma(\delta+1)}{\beta}t^{\beta}\right)\right], \tag{36}$$

for $>1/\sqrt{2}$. This solution represents a nonlinear periodic (elliptic) wave, where ϖ governs the transition from periodic behavior to a localized soliton.

Case 16: $h_1=\dfrac{1}{4}$, $h_2=\dfrac{1-2\varpi^2}{2}$ and $h_3=\dfrac{1}{4}$, then $F(\rho)=\dfrac{sn(\rho;\varpi)}{1+cn(\rho;\varpi)}$. In this case, Eq. (13) takes the form:

$$u(x,t)=\left(\frac{a_2}{3a_3}\pm\sqrt{\frac{a_2}{9(2\varpi^2-1)a_3^2}}\frac{sn\left(kx+\dfrac{\lambda\Gamma(\delta+1)}{\beta}t^{\beta};\varpi\right)}{1+cn\left(kx+\dfrac{\lambda\Gamma(\delta+1)}{\beta}t^{\beta};\varpi\right)}\right)\times\exp\left[i\left(\theta_1 x+\frac{\theta_2\Gamma(\delta+1)}{\beta}t^{\beta}\right)\right], \tag{37}$$

for $>1/\sqrt{2}$. This solution represents a nonlinear periodic wave, where ϖ controls the transition from sinusoidal to soliton behavior. We note that the limiting behavior of Jacobi elliptic functions (JEFs) is summarized in Table 1.

Table 1. Limiting forms of Jacobi elliptic functions as $\varpi\to 0$ and $\varpi\to 1$.

JEFs	$\varpi\to 0$	$\varpi\to 1$	JEFs	$\varpi\to 0$	$\varpi\to 1$
$sn(\rho;\varpi)$	$sin(\rho)$	$tanh(\rho)$	$dn(\rho;\varpi)$	1	$sech(\rho)$
$cs(\rho;\varpi)$	$cot(\rho)$	$csch(\rho)$	$sc(\rho;\varpi)$	$tan(\rho)$	$sinh(\rho)$
$cn(\rho;\varpi)$	$cos(\rho)$	$sech(\rho)$	$ns(\rho;\varpi)$	$csc(\rho)$	$coth(\rho)$
$ds(\rho;\varpi)$	$csc(\rho)$	$csch(\rho)$			

5. Discussion and influence of the M-truncated derivative

The obtained solutions reveal a wide variety of nonlinear wave structures governed by the Jacobi elliptic functions and their limiting forms. In particular, the solutions expressed in terms of sn, cn, and dn functions represent periodic wave patterns, where the modulus parameter ϖ controls the transition between periodic and solitary wave behaviors. As $\varpi \to 1$, these solutions reduce to hyperbolic forms such as $\tanh$ and sech, corresponding to kink-type and localized soliton structures, which are important in modeling stable wave propagation in nonlinear optics. Conversely, the limit $\varpi \to 0$ leads to trigonometric solutions, indicating oscillatory wave behavior. Moreover, the presence of different functional forms, such as *ns*, *dc*, *sd*, and combined structures, indicates the existence of singular, periodic-singular, and composite wave profiles, thereby enriching the model's dynamical features. These solutions describe various physical phenomena, including wave modulation, energy localization, and interaction patterns in nonlinear media.

A key observation from the graphical results is the significant influence of the fractional parameters β and δ, which arise from the M-truncated derivative. As β decreases, the wave profiles exhibit noticeable changes in amplitude, width, and propagation speed, indicating that the memory effect introduced by the fractional operator plays a crucial role in controlling wave dynamics. In particular, smaller values of β tend to slow down the wave evolution and modify the localization properties of the solitons. This behavior highlights the advantage of the M-truncated derivative over classical and other fractional operators, as it offers greater flexibility in tuning wave characteristics while maintaining analytical tractability.

Overall, unlike many existing studies that primarily report standard solution forms, the present results provide a broader spectrum of wave structures and a clear demonstration of how fractional effects influence their physical behavior. This not only enhances the understanding of the QC-NLSE model but also provides a more comprehensive framework for describing complex nonlinear wave phenomena.

The M-truncated derivative (MTD) is a mathematical operator introduced to incorporate memory and nonlocal effects in a fractional framework. It should be emphasized that the MTD is not a physical mechanism; rather, it is a modeling tool for describing fractional time dynamics.

In this context, the fractional parameters β and δ arising from the MTD formulation influence the temporal scaling and evolution of the solutions. These parameters modify the effective wave dynamics by controlling the rate of evolution and the solution's time scaling behavior. In particular, variations in β lead to changes in the propagation characteristics such as wave speed, width, and localization properties. This reflects the MTD's role as a tool for incorporating memory-dependent dynamics, rather than as a direct physical force or mechanism.

The influence of the M-truncated derivative (MTD) on the QC-NLSE (1) solutions is illustrated through two- and three-dimensional plots for selected parameter values. The solution profiles given by Eqs. (14), (15), and (17), shown in Figs. 1–3 correspond to different pulse types. In particular, they describe periodic wave trains, kink-type solitons, and bright solitary pulses, respectively. These profiles demonstrate the diversity of nonlinear excitations supported by the model under the effect of the fractional framework.

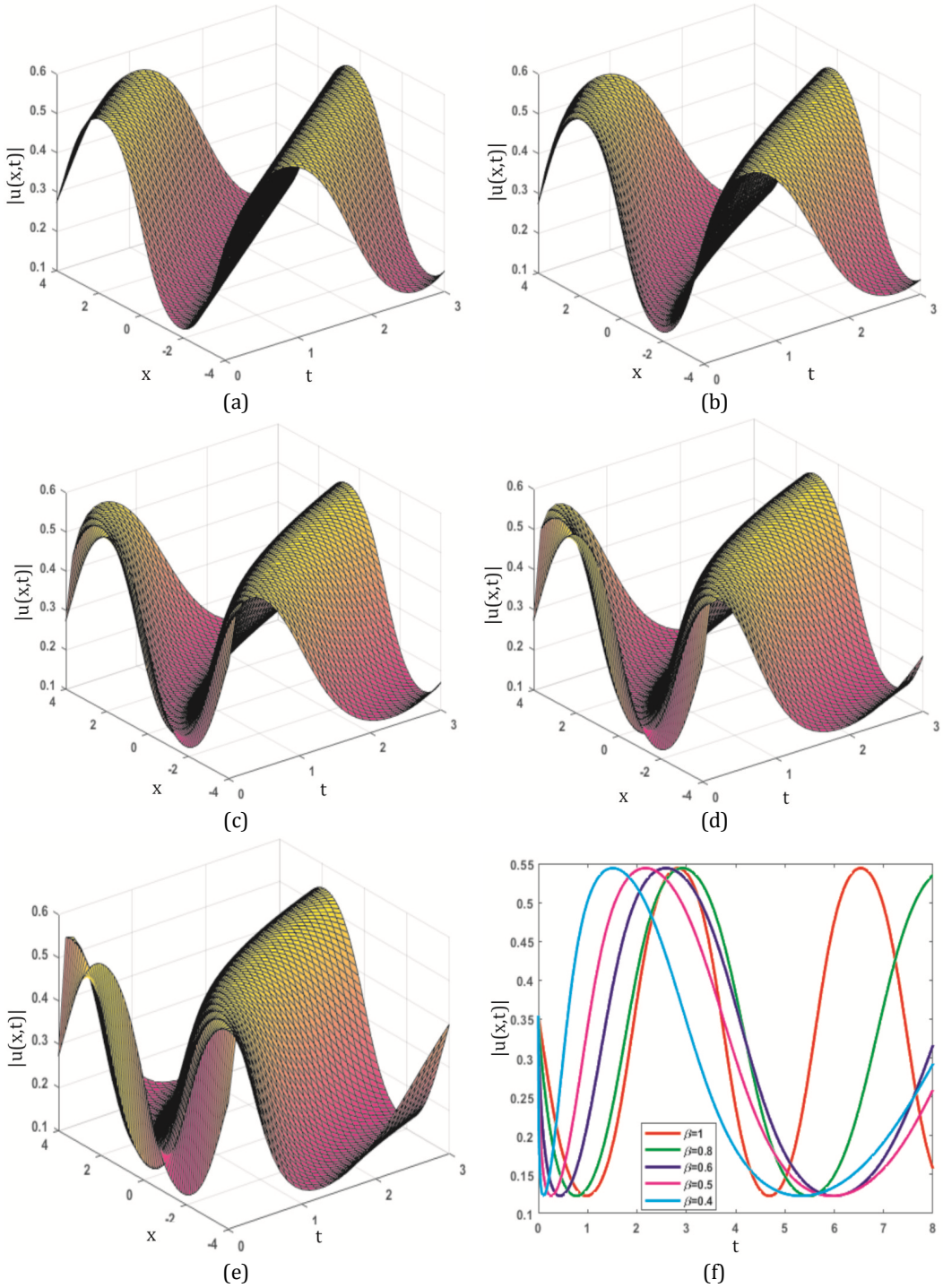

Fig. 1. (a-e) describe the 3D-profile of the amplitude $|u(x,t)|$ for Eq. (14), while (f) describes the 2D-profile of Eq. (14) with a distinct β. The parameter values are $\varpi = 0.5$, $a_2 = a_3 = k = 1$, $\lambda = -2$, with the ranges $-4 \le x \le 4$ and $0 \le t \le 3$. The fractional parameters are specified as follows: (a) $\beta = 1$, $\delta = 0$; (b) $\beta = 0.8$, $\delta = 0.9$; (c) $\beta = 0.6$, $\delta = 0.9$; (d) $\beta = 0.5$, $\delta = 0.9$; (e) $\beta = 0.4$, $\delta = 0.9$; and (f) $\beta = 1, 0.8, 0.6, 0.5, 0.4$ with δ =0.9.

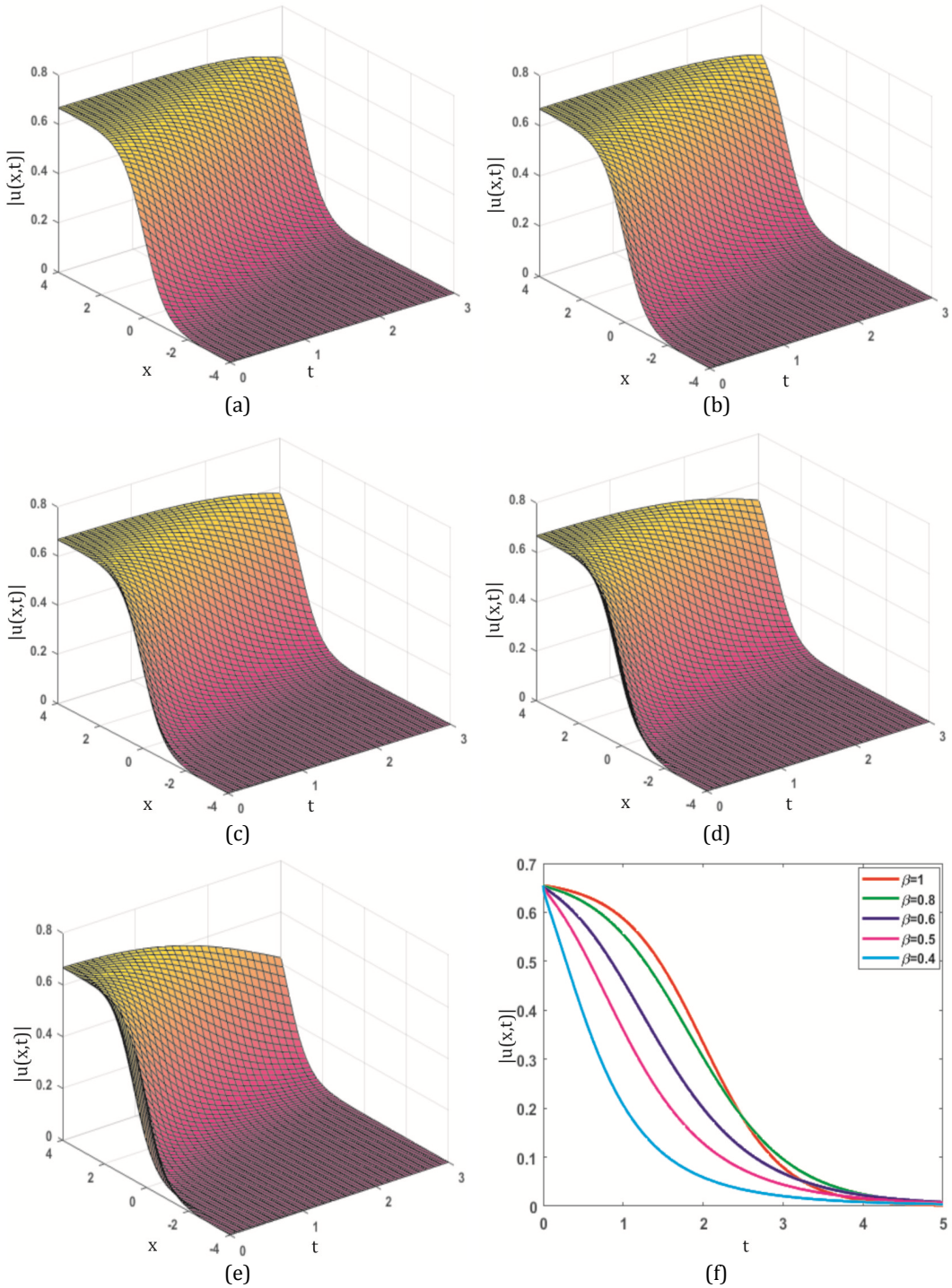

Fig. 2. (a-e) describe the 3D-profile of the amplitude $|u(x,t)|$ for Eq. (15), while (f) describes the 2D-profile of Eq. (15) with a distinct β. The parameter values are $a_2 = a_3 = k = 1$, $\lambda = -1$, with the ranges $-4 \le x \le 4$ and $0 \le t \le 3$. The fractional parameters are specified as follows: (a) $\beta = 1$, $\delta = 0$; (b) $\beta = 0.8$, $\delta = 0.9$; (c) $\beta = 0.6$, $\delta = 0.9$; (d) $\beta = 0.5$, $\delta = 0.9$; (e) $\beta = 0.4$, $\delta = 0.9$; and (f) $\beta = 1, 0.8, 0.6, 0.5, 0.4$ with δ =0.9.

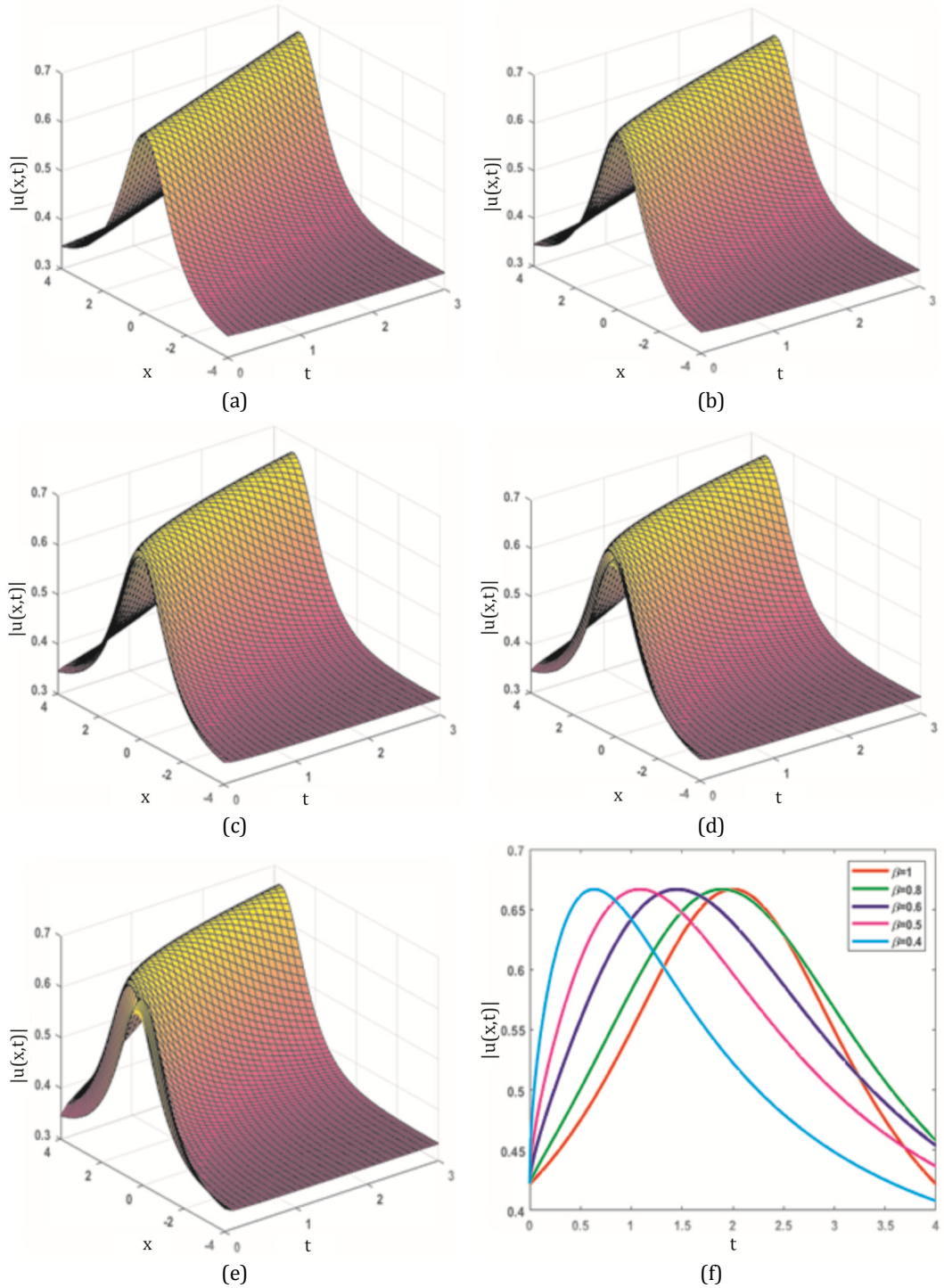

Fig. 3. (a-e) describe the 3D-profile of the amplitude $|u(x,t)|$ for Eq. (17), while (f) describes the 2D-profile of Eq. (17) with a distinct β. The parameter values are $a_2 = a_3 = k = 1$, $\lambda = -1$, with the ranges $-4 \le x \le 4$ and $0 \le t \le 3$. The fractional parameters are specified as follows: (a) $\beta = 1$, $\delta = 0$; (b) $\beta = 0.8$, $\delta = 0.9$; (c) $\beta = 0.6$, $\delta = 0.9$; (d) $\beta = 0.5$, $\delta = 0.9$; (e) $\beta = 0.4$, $\delta = 0.9$; and (f) $\beta = 1, 0.8, 0.6, 0.5, 0.4$ with δ =0.9.

Figs. 1-3 reveal the significant influence of accounting for the M-truncated derivative through the fractional parameter β on the evolution of the soliton structure. When β =1, the model reduces to the classical (integer-order) case with stable amplitude and smooth propagation along the spatial direction. The wave maintains its shape and travels without noticeable distortion, which is consistent with classical QC-NLSE dynamics.

When β decreases to β =0.8 and β =0.6, the influence of the fractional modeling through the M-truncated derivative becomes more apparent in describing the wave dynamics. The soliton begins to experience a slight deformation, in which its amplitude decreases slightly and its width increases.

For smaller values such as β = 0.5 and β = 0.4, the influence of fractional modeling becomes more pronounced. The soliton exhibits noticeable broadening, accompanied by a reduction in amplitude and slower propagation. The wave profile becomes more diffused, reflecting enhanced memory and nonlocal characteristics as described by the M-truncated derivative. This behavior suggests that the MTD effectively balances nonlinearity and dispersion, leading to weaker localization and enhanced damping-like behavior in the wave structure.

Overall, the results indicate that decreasing β leads to broader wave profiles with reduced amplitude and slower propagation. This behavior reflects enhanced memory and nonlocal interactions in the medium, which redistribute the wave energy over a wider region and delay its evolution. Such features are typical of fractional models and provide a more realistic description of wave dynamics in complex media compared to the classical integer-order framework.

6. Conclusion

In this work, the quadratic–cubic nonlinear Schrödinger equation with the M-truncated derivative has been investigated. By applying the F-expansion method, several classes of exact solutions were obtained in terms of Jacobi elliptic functions and their limiting forms, yielding elliptic, trigonometric, and hyperbolic wave structures. The obtained solutions were illustrated through two- and three-dimensional visualizations for selected parameter values, providing a clear description of their dynamical behavior. The influence of the fractional parameters was interpreted in terms of their contributions to the mathematical description of memory effects, with variations in β and δ leading to noticeable changes in wave amplitude, width, and propagation characteristics. These results provide a consistent analytical framework for describing complex wave patterns in the QC-NLSE model. Future work will investigate how different fractional operators affect the behavior of nonlinear wave solutions.

Acknowledgement. The researchers would like to thank the Deanship of Graduate Studies and Scientific Research at Qassim University for financial support (QU-APC-2026).

Authors contribution. Sofian T. Obeidat: conceptualization, resources, data curation, writing-review editing. Doaa Rizk: methodology, investigation, funding acquisition, writing-original draft. Wael W. Mohammed: software, data curation, visualization, writing-review editing.

Declaration of competing interest. The authors declare that they have no known competing financial interests or personal relationships that could have appeared to influence the work reported in this paper.

Data availability. All data generated or analyzed during this study are included in this article.

References

1. Oldham, K., & Spanier, J. (1974). *The fractional calculus theory and applications of differentiation and integration to arbitrary order* (Vol. 111). Elsevier.
2. Miller, K. S., Ross, B. (1993). *An Introduction to the Fractional Calculus and Fractional Differential Equations*, A Wiley-Interscience Publication, John Wiley & Sons, New York, NY, USA.
3. Podlubny, I. (1999). *Fractional Differential Equations*, vol. 198 of Mathematics in Science and Engineering, Academic Press, San Diego, Calif, USA.
4. Hilfer, R. (Ed.). (2000). *Applications of fractional calculus in physics*. World scientific.Oustaloup, A. (1991). La Commande CRONE: Commande Robuste d'Ordre Non Entier, Editions Herm_es, Paris, France.
5. Khan, K., Akbar M.A. (2014). The exp(-φ(ξ))-expansion method for finding travelling wave solutions of Vakhnenko-Parkes equation. *International Journal of Dynamical Systems and Differential Equations*, *5*(1), 72-83.
6. Baskonus, H.M., Bulut, H., Sulaiman T.A. (2019). New complex hyperbolic structures to the lonngren-wave equation by using sine-gordon expansion method. *Applied Mathematics and Nonlinear Science*, *4*, 129-138.
7. Yan, A (2003). Abunbant families of Jacobi elliptic function solutions of the dimensional integrable Davey-Stewartson-type equation via a new method. *Chaos Solitons Fractals*, *18*, 299-309.
8. Lu, B. (2012). The first integral method for some time fractional differential equations. *Journal of Mathematical Analysis and Applications*, *395*, 684-693.
9. Jiong, S. (2003). Auxiliary equation method for solving nonlinear partial differential equations. *Physics Letters A*, *309*, 387-396.
10. He, J.H., Wu, X.H. (2006). Exp-function method for nonlinear wave equations. *Chaos Solitons Fractals*, *30*, 700-708.
11. Wang, M.L., Li, X.Z., Zhang, J.L. (2008). The (G'/G)-expansion method and travelling wave solutions of nonlinear evolution equations in mathematical physics. *Physics Letters A*, *372*, 417-423.
12. Zhang, H. (2009). New application of the (G'/G)-expansion method. *Communications in Nonlinear Science and Numerical Simulation*, *14*, 3220-3225.
13. Wazwaz, A.M. (2004). The sine-cosine method for obtaining solutions with compact and noncompact structures. *Applied Mathematics a Computation*, *159*, 559-576.
14. Attia, R. M. A., Khater, M. M. A., Ahmed, A. E., El-Shorbagy, M. A. (2011). Accurate sets of solitary solutions for the quadratic-cubic fractional nonlinear Schrödinger equation. *AIP Advances*, *11*, 055105.
15. Badshah, F., Tariq, K. U., Zeeshan, M., Ahmad, H., Ismail, G. M., Khedher, K. M. (2024). On the dynamical study of the quadratic-cubic fractional nonlinear Schrödinger model in superfast fibers. *Optical and Quantum Electronics*, *56*, 822.
16. Islam, M.T., Aktar, M.A., et al. (2021). Further innovative optical solitons of fractional nonlinear quadratic-cubic Schrödinger equation via two techniques. *Optical and Quantum Electronics*, *53*, 562.
17. Riesz, M. (1939)). L'intégrale de Riemann-Liouville et le problème de Cauchy pour l'équation des ondes. *Bulletin de la Société Mathématique de France*, *67*, 153-170.
18. Wang, K.L., Liu, S.Y. (2016). He's fractional derivative and its application for fractional Fornberg-Whitham equation. *Thermal Science*, *1*, 54-54.
19. Miller, S., Ross, B. (1993). *An introduction to the fractional calculus and fractional differential equations*. Wiley, New York, NY, USA.
20. Caputo, M., Fabrizio M. (2015). A new definition of fractional differential without singular kernel. *Progress in Fractional Differentiation & Applications*, *1*(2), 1-13.
21. Sousa, J.V., de Oliveira, E.C. (2018). A new truncated Mfractional derivative type unifying some fractional derivative types with classical properties. *International Journal of Analysis and Applications*, *16*(1), 83-96.
22. Peng, Y. Z. (2004). Exact periodic wave solutions to the coupled Schrödinger-KdV equation and DS equations. *Pramana*, *62*(4), 933-941.
23. Zhang D. (2005). Doubly periodic solutions of the modified Kawahara equation. *Chaos Solitons Fractals*, *25*(5), 1155-1160, 2005.
24. Liu, Q., Zhu, J.-M. (2006). Exact Jacobian elliptic function solutions and hyperbolic function solutions for Sawada-Kotere equation with variable coefficient. *Physics Letters A*, *352*(3), 233-238.

Obiedat, S. T., Rizk, D., Mohammed, W. W. (2026). Investigation of New Optical Solutions of the Fractional Schrödinger Equation with Accounting for Third-Order Nonlinearity. *Ukrainian Journal of Physical Optics*, *27*(3), 03083 – 03099.
doi: 10.3116/16091833/Ukr.J.Phys.Opt.2026.03083

Анотація. *У цій статті ми розглянули квадратично-кубічне нелінійне рівняння Шредінгера (КК-НРШ), сформоване за допомогою М-усіченої похідної (МПД). Використовуючи метод F-розкладу, отримано різноманітні точні аналітичні розв'язки, включаючи періодичні, яскраві, кінкові, антикінкові, сингулярні та темні солітонні структури. Показано, що метод є системним та ефективним для побудови точних розв'язків нелінійних еволюційних рівнянь з характеристиками дробового порядку. Основний внесок цієї роботи полягає у виведенні та класифікації різноманітної родини хвильових розв'язків для КК-НРШ з МПД. Графічне моделювання виконано за допомогою MATLAB для ілюстрації впливу дробового параметра на поведінку отриманих розв'язків. Результати показують, що варіації цього параметра призводять до помітних змін у формі та особливостях поширення хвильових структур, тоді як аналітичний метод служить інструментом для опису цих властивостей.*

Ключові слова: *М-усічена похідна, оптичні солітони, моделювання, метод F-розкладу, квадратично-кубічні нелінійні еволюційні рівняння*